J Mater Sci: Mater Electron (2023) 34:1577

Synthesis of novel biodegradable starch-PMA and Ag@starch-PMA polymer composite for boosting charge separation ability and superior photocatalytic performance

Muhammad Amjad[1], Ayesha Mohyuddin[1], Mohsin Javed[1], Shahid Iqbal[2,*], Rabia Liaquat[3], Mohammed T. Alotaibi[4], Wajad Ulfat[1], Randa A. Althobiti[5], Eman Alzahrani[6], Abd-ElAziem Farouk[7], Murefah Mana Al-Anazy[8], and Eslam B. Elkaeed[9]

[1] Department of Chemistry, School of Science, University of Management and Technology, Lahore 54770, Pakistan
[2] Department of Chemistry, School of Natural Sciences (SNS), National University of Science and Technology (NUST), H-12, Islamabad 46000, Pakistan
[3] Energy Systems Engineering Department, U.S.-Pakistan Center for Advanced Studies in Energy (USPCAS-E), National University of Sciences and Technology (NUST), Islamabad 44000, Pakistan
[4] Department of Chemistry, Turabah University College, Taif University, P.O. Box 11099, Taif 21944, Saudi Arabia
[5] Department of Chemistry, College of Science, University of Bisha, P.O Box 511, Bisha 61922, Saudi Arabia
[6] Department of Chemistry, College of Science, Taif University, P.O. Box 11099, Taif 21944, Saudi Arabia
[7] Department of Biotechnology, College of Science, Taif University, P.O. Box 11099, Taif 21944, Saudi Arabia
[8] Department of Chemistry, College of Science, Princess Nourah bint Abdulrahman University, P.O. Box 84428, Riyadh 11671, Saudi Arabia
[9] Department of Pharmaceutical Sciences, College of Pharmacy, AlMaarefa University, Riyadh 13713, Saudi Arabia

Received: 8 April 2023
Accepted: 13 July 2023
Published online:
24 July 2023

ABSTRACT

One of the main issues confronting researchers is the removal of hazardous organic dyes from industrial effluent. In this work, a biodegradable starch-based polymer (starch-PMA) and silver blend (Ag@starch-PMA) nanocomposite were developed by a free radical process and employed as adsorbents for efficiently removing the hazardous dyes from industrial wastewater. The synthesized polymer adsorbent's ability to bind to the methylene blue dye in water was tested under optimal conditions. The techniques, including FTIR, indicate the functional groups, TGA/DTG provide the thermal degradation of Ag@starch-PMA (76%) and starch-PMA (90%) at 520 °C and 500 °C, respectively. The surface morphology of the composites was investigated using SEM, and their biodegradation was examined using the soil burial technique. Further, in the adsorption process, parameters like adsorbent dose (0.15 g), pH range (2–12), and dye solution concentration (10 ppm) are optimized. The experimental data indicate the adsorption efficiency of Ag@starch-PMA (95%) and starch-PMA

Address correspondence to E-mail: shahidgcs10@yahoo.com

https://doi.org/10.1007/s10854-023-10997-4

(92%) under the basic pH (8.4–10.4) and further remains constant. The q_{max} of starch-PMA (522.7834 mg/g) and Ag@starch-PMA (541.2563 mg/g) were assessed by Freundlich adsorption isotherm. In addition, linear fitting kinetic data of starch-PMA (R^2 = 0.8619) and Ag@starch-PMA (R^2 = 0.9898) showed that the adsorbents follow the pseudo-first order and pseudo-second order of reaction, respectively. A unique adsorbent for the removal of MB dye from an aqueous solution may therefore be found in the resultant nanocomposite.

1 Introduction

Human society and devolving industries are the two main factors generating environmental pollution. The various industries such as paints, cosmetics, food, textile, leather, mining, pharmaceutical, and chemical manufacturing release industrial effluents containing heavy metal ions, dyes, and non-biodegradable materials that deteriorate the quality of water and disturb aquatic life [1–4]. Dyes pose serious problems since 10–15% of them are lost during processing and lead to eutrophication [5, 6]. The dye concentration (> 2 ppm) in water proves to be toxic and may cause vomiting, diarrhea, gastritis, headache skin irritation and also affects the photosynthesis process by less diffusion of light in water. To protect wildlife, it is thus a worldwide issue to remove the dyes from industrial effluents [7]. Several techniques have been utilized for the treatment of industrialized effluents like chemical precipitation [8], electrocoagulation, oxidation, ozonation, reverse osmosis [9], photocatalytic degradation [10], and adsorption [11]. Therefore, there is an urgent need to develop regenerative and eco-friendly technologies to tackle environmental problems.

The most efficient technique is adsorption due to its flexibility in a wide range of dyes, simple design, low cost, easy operation, and high efficiency [12, 13]. Generally, to remove the pollutants from industrial wastewater mostly activated carbon as an adsorbent is used due to wide properties like porous high surface area and surface reactivity [14, 15]. Although, its utilization on a wide scale makes it difficult due to dispersion, cost-effectiveness, and reusability [16, 17]. Over the last decade, numerous materials like polymer resins [18], clay minerals [19], nanotubes [20], nanofibers [21], metal oxide and polymer-based nanomaterials [22] have been utilized for the treatment of industrial waste discharges. The adsorbents such as lemon peel, peach stones, coffee bean, walnut wood, and rice husk have also been reported for dye adsorption [23–26]. These described adsorbent's sluggish kinetics make them undesirable. Biopolymer composites have drawn a lot of interest because of their distinctive qualities, including oxygen permeability, low interfacial tension, and biodegradation [27, 28]. The unmodified biopolymer materials have weak mechanical strength, lack reusability, and high solubility in water, that's why cannot be repeatedly used as adsorbent material [29]. By grafting various monomers onto the polymer's backbone and adding metal nanoparticles (MNPs) like Ni, Ag, Au, CNT, and graphene to increase their mechanical strength, unmodified biopolymers may be changed. MNP's high surface energy and surface area are what cause the dye molecules to adhere to the polymer surface [30, 31].

Numerous studies have been reported against adsorbents for dye removal, guar gum (GG) natural polysaccharide grafted carbon nanotubes with an adsorption capacity of 61.92 mg/g [32–34], GG/poly(AA) and GG/poly(AA-in-ANI) are 167.571 and 168.577 (mg/g) [35], Chitosan/PVP/Bi2O3 nanocomposite, composite films made of chitosan-based natural products (ginger, curcumin, and cinnamon) as biomaterials, and chitosan-zinc oxide (ZnO) nanocomposite are only a few examples. Xanthan gum was grafted with acrylamide containing nano-silica [36]. The observed concentrations of the hydrogel polymer based on gg-cl-P(AAm-co-MAA) are 497.5 mg/g and 694.44 mg/g, respectively. But metallic composites like $CoFe_2O_4$@CMC/HZSM-5 are also helpful for treating wastewater [37]. The utilization of starch-grafted polymer composites (starch-PMA and Ag@starch-PMA) as an adsorbent material is so far to be explored. The AgNPs show remarkable photocatalytic dye degradation efficiency the rationale to blend with starch-PMA composite to enhance the adsorption efficiency and gained significant interest in dye removal from industrial wastewater [38]. The challenges regarding the MB removal from aqueous solution using these polymers as adsorbent is still required.

In the present work, innovative biodegradable Starch-PMA and Ag@Starch-PMA polymer composites that are eco-friendly, affordable, and biodegradable were created for the efficient removal of MB from wastewater. To our best knowledge, synthesized starch-based polymers have not been reported. In addition, the effects of pH, contact duration, dosage, adsorbent and dye concentration were examined. The adsorption of MB in an aqueous solution has also been evaluated using kinetic models and isotherms.

2 Materials and methods

2.1 Materials

Starch [M = 342.30 $(C_6H_{10}O_5)n$, 99%, Sigma], acrylic acid (AA) ($C_3H_4O_2$, 97%, DOW Chemical Company), methyl methacrylate (MMA) ($C_5H_8O_2$, 98%, DOW Chemical Company), Lactic Acid (LA), (98%, DOW Chemical Company), Lutensol XL-100 (alkyl polyethylene glycol ethers, 97%, Sigma), potassium persulphate ($K_2S_2O_8$, 99%, Sigma), AgNPs (97%, Sigma), distilled water and commercial Methylene blue dye ($C_{16}H_{18}ClN_3S$). Analytical grade substances were used throughout the whole experimental process.

2.2 Synthesis of starch-PMA and Ag@starch-PMApolymer composite

0.5 g of starch was dissolved in 50 mL of distilled water at 85 °C in a three-necked reaction kettle with a mechanical stirrer to create a translucent solution. After 25 min, the starch solution was combined with Lutensol XL 100 (0.5 g) as an emulsifier and potassium persulphate (0.15 g) as an initiator (5 min). The initiator generates the free radicals of starch functional groups that start the polymerization reaction. Following that, a combination of pure monomers (4 mL of methyl methacrylate, 4 mL of acrylic acid, and 2 mL of polylactic acid) was added at a rate of one milliliter per minute while vigorously stirring the mixture and the temperature was maintained for one hour. Next, 0.005 g of green synthetic AgNPs were added, and the reaction was allowed to run its course for 30 min while being stirred. In the end, the reaction mixture was left over at room temperature; a very fine thin film of Starch-PMA and Ag@starch-PMA was obtained.

2.3 Characterization of starch-PMA and Ag@starch-PMA polymer composites

The presence of NPs inside the Ag@starch-PMA polymer composite is confirmed by UV–Vis absorption spectra (Shimadzu, UV-1240, Kyoto, Japan) in the range 300–700 nm at ambient temperature. To confirm the grafting of monomers on the starch backbone, the synthesis of starch-PMA and Ag@starch-PMA polymer composites and to examine their chemical composition FTIR (Midac Corporation) spectrum is recorded (4000–500 cm^{-1}). The morphology of synthesized composite thin films is examined using SEM (Nova NanoSEM 450 field-emission) and the presence of the AgNPs was confirmed by the EDX analysis. A heating rate of 10 °C/min was used to measure the TGA/DTG (SDT Q600 V20.9) analysis.

2.4 Dye adsorption studies

2.4.1 Preparation of MB stock solution

A stock solution was made by dissolving 1 g of MB in 1 L of distilled water. Before using the stock solution to make the solutions for the adsorption research, it was diluted to the required concentration. To adjust the mixture's pH, either 1 M NaOH or 1 M HCl was added.

2.4.2 Dye adsorption experiment

The purpose of the adsorption experiment was to examine how the MB adsorbs to starch-PMA and Ag@starch-PMA. Examined separately were the effects of contact duration, adsorbent dosage, starting dye concentration, and solution pH. Using a UV-Vis spectrophotometer (UV-1800, Shimadzu Corporation, Japan) that operates in the 400–800 nm range, the concentration of the MB aqueous solution was assessed both before and after adsorption. The MB solution (250 mL) was taken in two flasks, and 0.15 g of each adsorbent was mixed and put on a thermostat shaker at 150 rpm. After that, the sample was taken every 5 min until the disappearance of the dye color. To determine the adsorption (percent) and capacity for MB, Eqs. (1) and (2) were utilized.

$$\text{Dye adsorption}(\%) = C_0 - \frac{Ce}{C_0} \times 100 \quad (1)$$

$$qt = \frac{C_0 - Ct}{m} \times V \quad (2)$$

Here, C_0 (mg/L), and Ce (mg/L) were MB concentration at the initial and at time t, respectively; V(L) volume of dye solution and m (g) weight of the polymer adsorbent used.

Initially, the effect of adsorbent dose starch-PMA and Ag@starch-PMA on MB solution (1 mg/L)was first studied. 0.15 g of starch-PMA and Ag@starch-PMA were introduced to MB solution (1 mg/L) at 298 K to evaluate the influence of pH (1.4–10.4) on dye removal. Next, a 1 M NaOH and 1 M HCl solution was used to adjust the pH of the mixture. The final solution was analyzed at equilibrium after 3 h and 15 min. The kinetic study was conducted with starch-PMA and Ag@starch-PMA in 250 mL of MB solution (1 mg/L) at 298 K, pH 8.4, and an adsorbent dose (0.15 g). At 298 K and pH 8, 0.15 g of starch-PMA and Ag@starch-PMA were added to 100 mL of MB at various starting concentrations (10, 100, 200, 300, 400, and 500 ppm) to create the adsorption isotherm.

3 Results and discussion

3.1 FTIR analysis

Figure 1A illustrates the FTIR spectra and represents the various peaks of functional groups in pure starch, AA, MMA, and LA, respectively. The broadband in the range 3400–3600 cm^{-1} and peak at 2950 cm^{-1} confirms the –OH and –C–H stretching vibration [39–41]. The strong peak at 2150 cm^{-1} and 1750 cm^{-1} and 1125 cm^{-1} is correlated with the C = C, –C = O, and –C–O extending vibrations in the monomers [42, 43]. Figure 1B showed the FTIR spectra of Starch-PMA and Ag@starch-PMA and AgNPs. The broadband in the range 3400–3600 cm^{-1} ascribed –OH, at 3150 cm^{-1}, –C = CH, below 3000 cm^{-1} –C–H, and 2150 cm^{-1} –C = CH stretching vibrations, respectively. Meanwhile, the distinctive peak at 1713 cm^{-1} appeared due to extending vibration of –C = O and ester groups. However, the FTIR spectrum of both prepared composites indicates that no additional peak was observed, and it suggests the Ag NPs interaction with polymer composites without any chemical bonding [44]. Therefore, we suggest that the AgNPs free network and anchored on the composite surface. So, these preliminary findings suggest that both composites had been manufactured.

3.2 Thermogravimetric analysis

The TGA-DTG analysis curves of Ag@starch-PMA(A-1) and Starch-PMA(A-2) polymer composites are represented in Fig. 2. The weight loss of prepared polymer composites was seen in three steps. The first stage, which occurs between 100 and 250 °C, is characterized by weight loss brought on by water molecules evaporating. In the second step, rapid thermal degradation of the organic content (polysaccharides and elimination of CO and CO_2) of prepared polymer composites occurs at 250–410 °C along with a small hump near 400 °C. The side chain and remaining AgNPs are degraded in the third stage, which starts at 410 °C and steadily decreases in weight until 600 °C. There is a slight difference in thermal degradation between Ag@starch-PMA (76%) and Starch-PMA (90%) at 520 °C and 500 °C, respectively, which is due to the presence of AgNPs.

3.3 SEM analysis

The parent composite, starch-PMA, and its silver-based nanocomposite, Ag@starch-PMA, are studied using the SEM method to examine the surface morphology and compatibility of AgNPs. Figure 3A–C represents the SEM images of the starch-PMA composite and it can be seen that rough, stratified surface with few folding and voids. Moreover, the incorporation and uniform dispersion of AgNPs in starch-PMA, a significant change in the morphology of polymer composite and leads to the improvement in the surface area shown in figure (D) and (E). Due to surface modification, the adsorption site for MB was enhanced on the surface of the Ag@starch-PMA polymer composite and showed excellent adsorption efficiency at room temperature.

Figure 4a displays the X-ray diffraction patterns of starch-PMA and Ag@starch-PMA composites. All Ag@starch-PMA composites exhibit the distinctive peaks of the starch with no discernible variations from pure starch. In the Ag@starch-PMA composites,

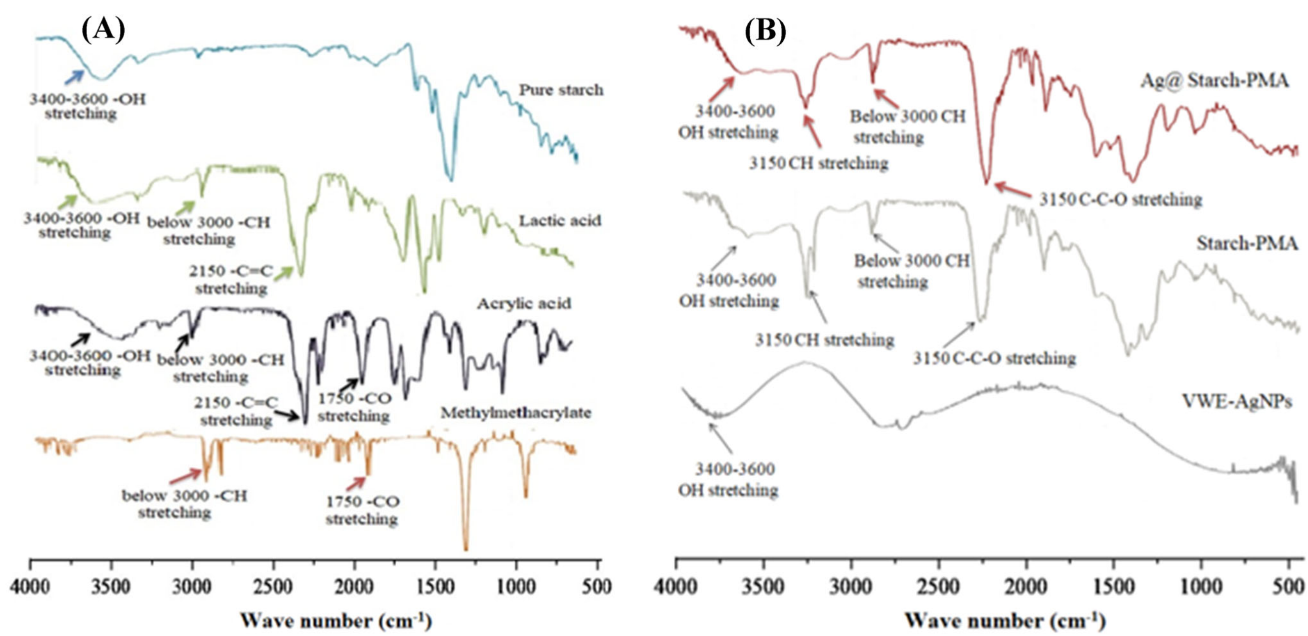

Fig. 1 **A** FTIR spectra of pure starch, monomers (PLA, AA, and MMA). **B** AgNPs, Starch-PMA, and Ag@starch-PMA polymer composites

diffraction peaks at 38.11°, 44.39°, 65.06°, and 77.51° are clearly discernible. These peaks are indexed with the card number (JCPDS#00-04-0783), and they correlate to the silver's face-centered cubic crystallographic planes (111), (200), (220), and (311). The coexistence of starch-PMA and Ag NPs as well as the construction of composites including Ag@starch-PMA were verified by XRD analysis (Fig. 4a) of the two materials. According to Fig. 4b, the BET surface areas for the starch-PMA and Ag@starch-PMA composites are 11.29 and 25.13 m^2/g, respectively. It was observed that whereas Ag@starch-PMA has a large BET surface area due to its composite structure, starch-PMA has a smaller BET surface area. Ag NPs generate a porous environment for efficient material synthesis as shown by the considerable enhance in BET surface area that results from the addition of Ag to the Ag@starch-PMA composite. The number of reaction active sites increases with BET surface area, which may be beneficial for enhancing adsorption efficacy.

3.4 Biodegradation studies

Using the soil burial technique, the biodegradation study of the polymer composites Starch-PMA and Ag@starch-PMA was investigated. Both composites underwent an 11 week burial test. Initially, the weight of both polymer composites increases due to water absorption present in the soil, and then gradually weight loss was observed. The polymer composite (Ag@starch-PMA) slightly shows less biodegradation due to the antimicrobial effect of AgNPs. The biodegradation of starch-PMA increased up to 37.79% while Ag@starch-PMA was 36.92% shown in Fig. 5.

3.5 Adsorption study of MB

3.5.1 Adsorption mechanism of MB dye onto polymer composites

The most feasible mechanism for MB adsorption on the surface of starch-PMA and Ag@starch-PMA polymer composites as adsorbents is shown in Fig. 6. The FTIR analysis examines the surface of composites formed of polymer materials to see whether functional groups (–OH and –COOH), which are essential to the adsorption process, are present. In the basic media of MB, both the –OH and –COOH are deprotonated [45]. A negative charge and a strong association with cationic MB are present on the polymer composite's surface, which is absorbed on the adsorbent surface. In addition, the interactions exist between electronegative atoms of polymer adsorbents and positive atoms of MB dye shown in Fig. 6.

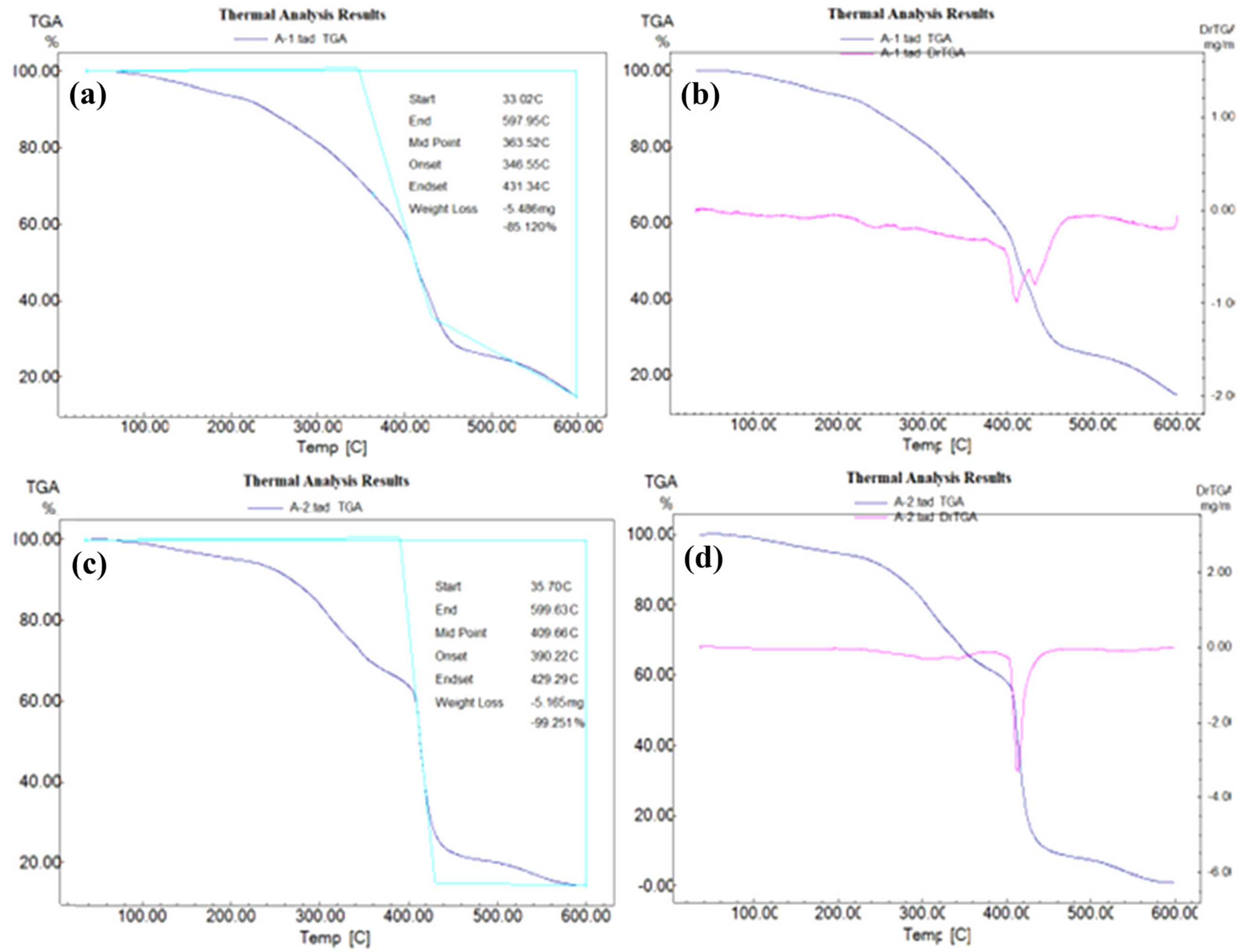

Fig. 2 **a** and **b** TGA-DTA plots of Ag@starch-PMA (A-1) and **c**, **d** Starch-PMA (A-2) polymer composite samples

Additionally, the AgNPs reinforced in the polymer composites increase the surface and provide surface energy to improve the likelihood that MB dye molecules will bind. Therefore, the surface of the produced adsorbent absorbs MB molecules.

3.5.2 *Aqueous solution MB dye absorption is affected by pH*

The pH of the MB dye solution has a major influence on the binding sites of the adsorbent in the adsorption process [46]. Throughout the adsorption process, the pH of the MB dye solution has a substantial influence on the adsorbent's binding sites [47, 48]. Therefore, the adsorption behavior of the synthesized starch-PMA and Ag@starch-PMA polymer composites for MB dye solution were studied by adjusting the pH range 1.4–12.4 at room temperature using 1 M HCl or 1 M NaOH. It is evident that an increase in pH results in an enhanced adsorption capacity for both polymer composites at equilibrium. Because MB dye is cationic and produces positive ions in an aqueous solution that stays constant up to pH12.4, it is noted that the highest adsorption of MB dye is reached at pH 7.4–8.4, as illustrated in Fig. 7. It is evident that an increase in pH results in an enhanced adsorption capacity for both polymer composites at equilibrium. Because MB dye is cationic and produces positive ions in an aqueous solution that stays constant up to pH12.4, it is noted that the highest adsorption of MB dye is reached at pH 7.4–8.4, as illustrated in Fig. 7.In acidic media ($pH < 7$), the polymer composite surface possesses positive charges due to the protonation of COO^- to COOH groups of the polymer chain which affect the adsorbent efficiency and retards its adsorption capacity but

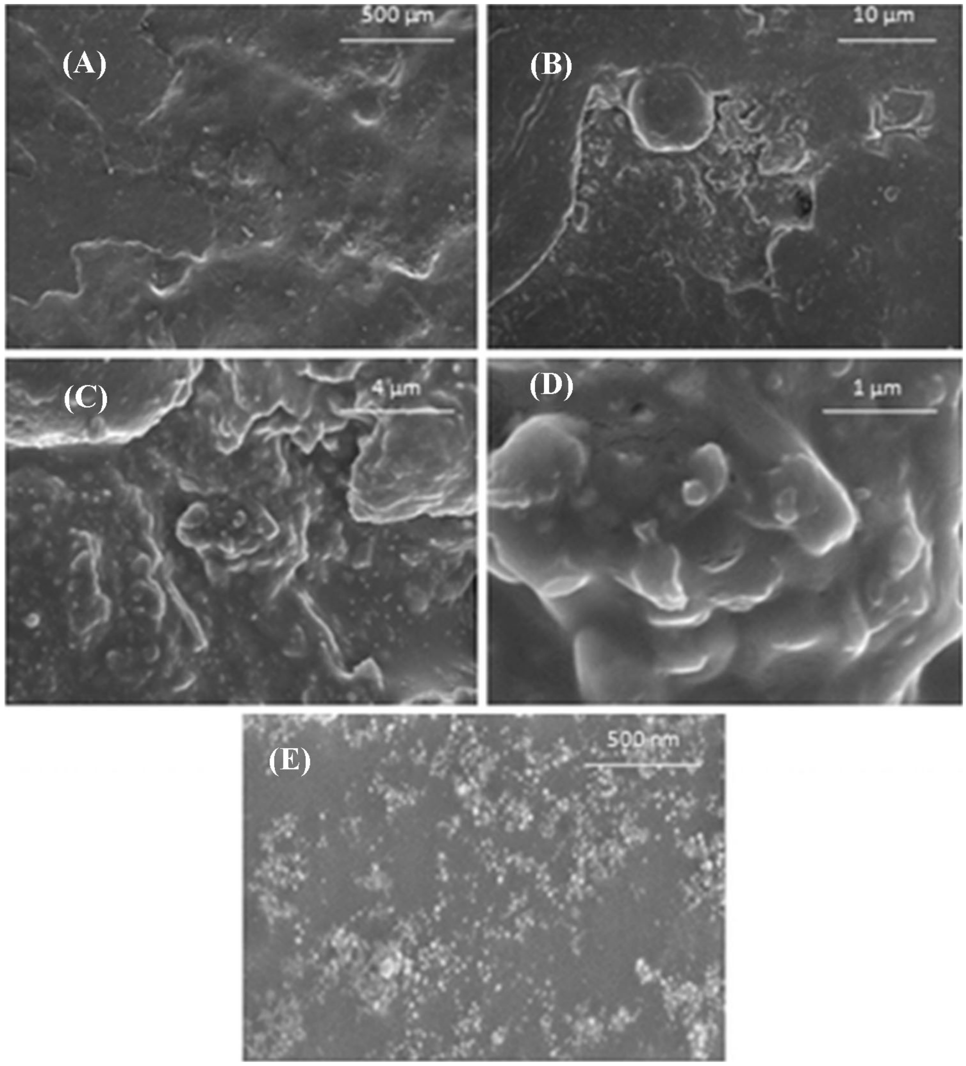

Fig. 3 SEM images of starch-PMA at **A** 500 µm, **B** 4 µm, **C** 10 µm and Ag@starch-PMA polymer composite at **D** 1 µm, **E** 500 nm

increases in pH value (9–13), COOH group ionize to COO^-, the polymer composite surface acquires a negative charge that enhances the adsorption process. As shown in Fig. 6, the electrostatic interaction between positive ions of MB dye and negative charges on the surface of the polymer composites supports the adsorption of Ag@starch-PMA and Starch-PMA on the surface of the polymer composites.

3.6 Adsorption kinetics studies

3.6.1 *Effects of adsorption kinetics and contact time*

The findings of the MB dye (1 mg/L) adsorption kinetics in the produced Starch-PMA and Ag@starch-PMA polymer composites are shown in Fig. 8a. According to the contact duration and MB removal for the two polymer composites, the adsorption rose quickly. The removal of dye is caused by the attachment of MB from the aqueous solution to the surface of polymer composites when shaken continuously. Comparing the results of two polymer composites, it can be observed that on equilibrium the adsorption of MB on Ag@starch-PMA is relatively higher than Starch-PMA. However, under the same adsorption condition (time 195 min and ambient temperature), the adsorption process reaches equilibrium in less time with higher adsorption on Ag@starch-PMA due to AgNPs. Following a 15 min dye adsorption procedure, all samples were collected and subjected to a UV/Vis spectrophotometer analysis between 300 and 700 nm.

The MB adsorption recycling tests with Ag@starch-PMA composites were conducted three times under the same reaction conditions since the stability of Ag@starch-PMA polymer composites is essential to

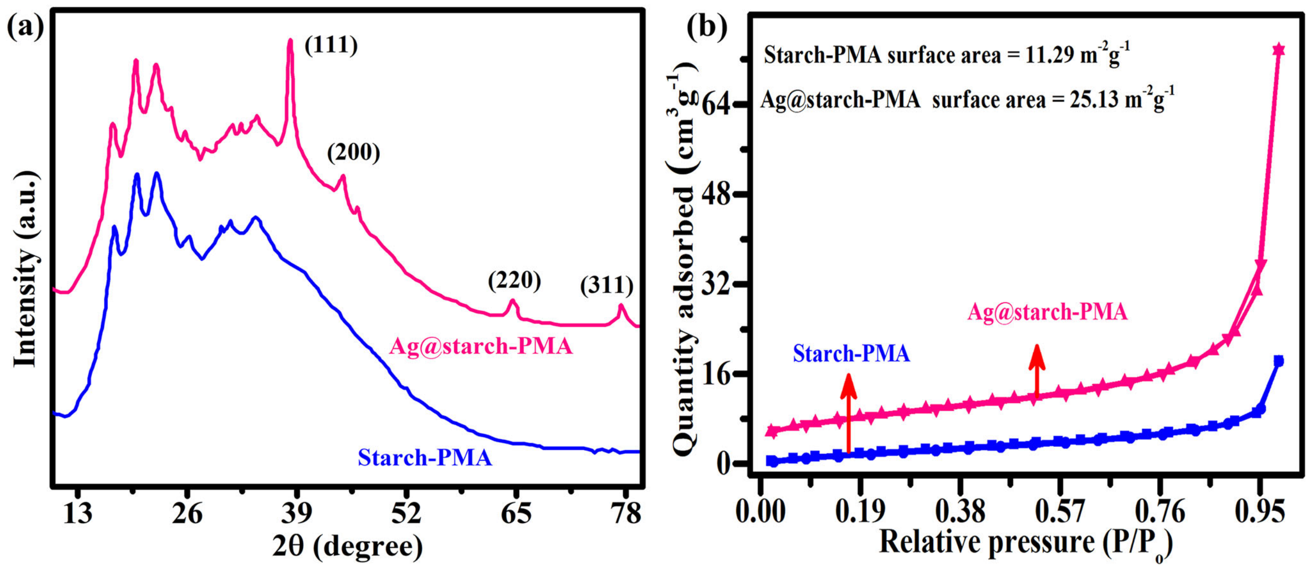

Fig. 4 **a** XRD pattern of starch-PMA and Ag@starch-PMA and **b** Nitrogen adsorption–desorption isotherms of starch-PMA and Ag@starch-PMA

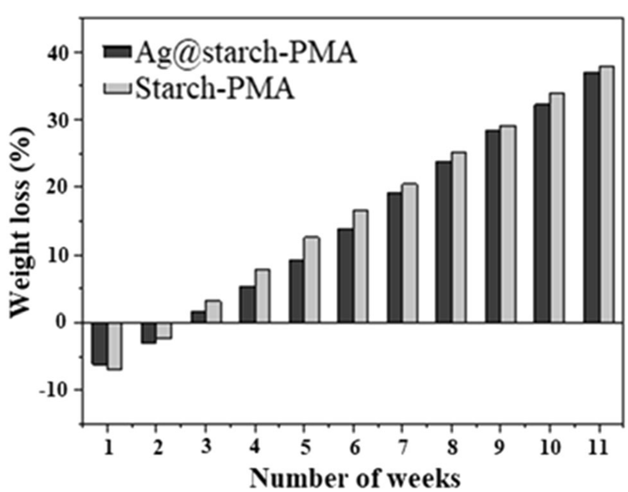

Fig. 5 Weight loss of Ag@starch-PMA and Starch-PMA polymer composites study by soil burial method

determining their appropriateness for practical applications. Figure 8b, c show, respectively, the XRD patterns of Ag@starch-PMA polymer composites before the reaction and after the third round of MB adsorption studies. The structural integrity of Ag@starch-PMA polymer composites is further confirmed by the absence of any visible structural changes between the time of adsorption recycling studies and the time prior. We may infer from the research above that the combination of Ag@starch and PMA polymer is a very durable and efficient adsorbent.

Fig. 6 Adsorption mechanism of MB on the surface of polymer composite

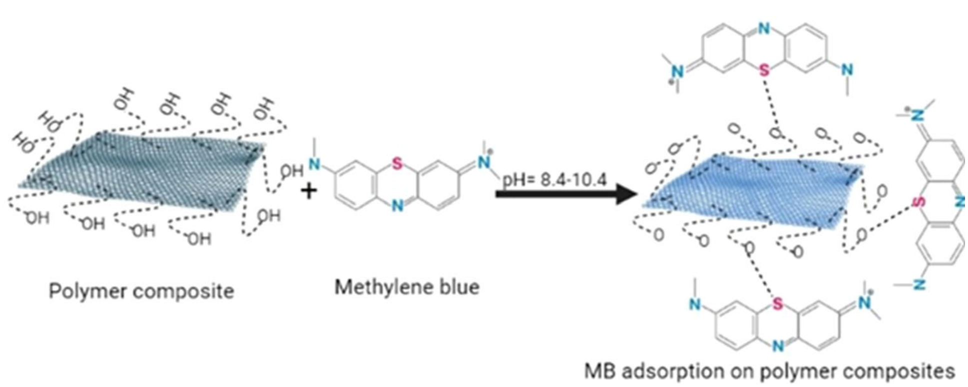

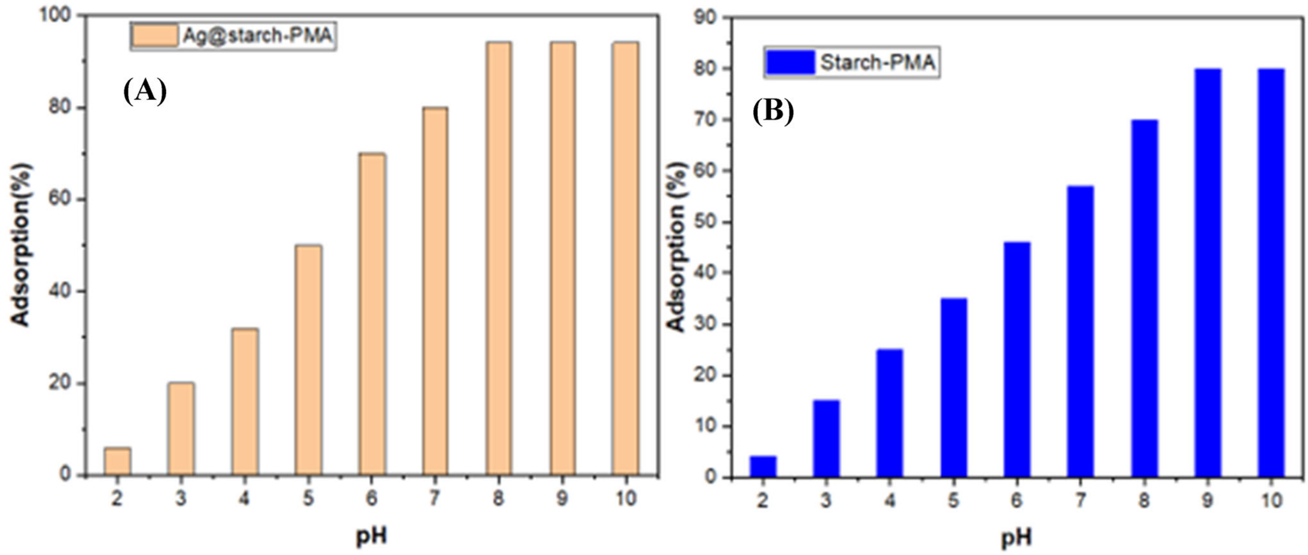

Fig. 7 Effect of pH on MB adsorption **a** Ag@starch-PMA and **b** Starch-PMA polymer composite

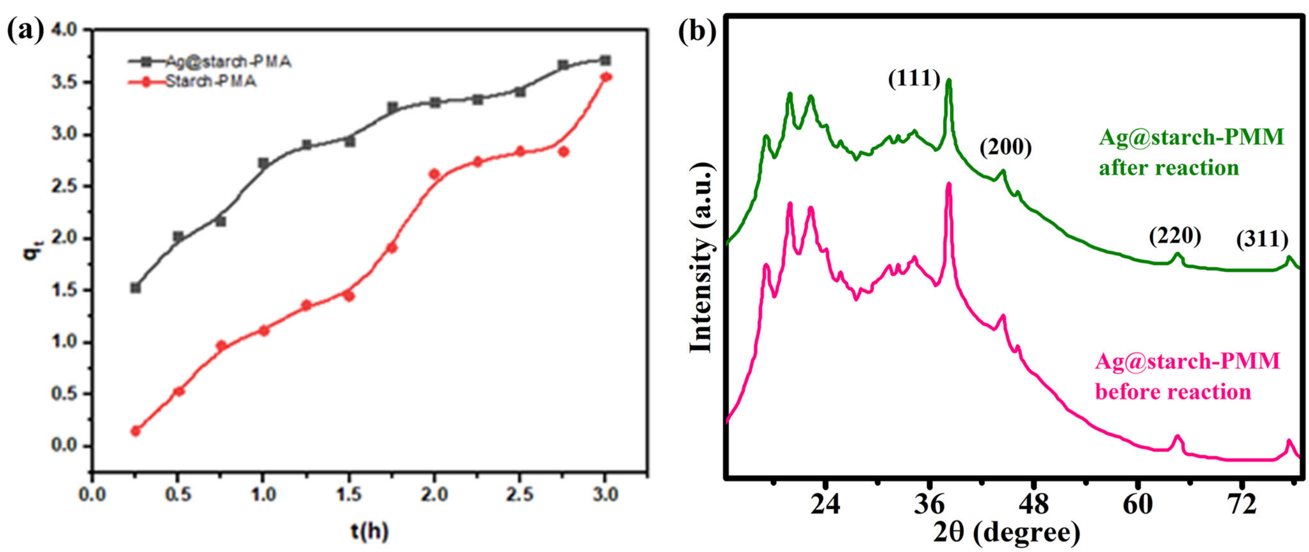

Fig. 8 **a** Effect of time on the amount of MB adsorbed onto Starch-PMA and Ag@starch-PMA polymer nanocomposites and **b** Structural stability of Starch-PMA and Ag@starch-PMA

3.6.2 Kinetic models

Figure 9 illustrates the MB adsorption kinetics toward the starch-PMA and Ag@starch-PMA. Using pseudo-first order and pseudo-second-order, the rate constant for MB may be written as [49, 50]:

$$\log(qe - qt) = \log qe - \left(\frac{\mathrm{K1}}{2.303}\right)t \quad (3)$$

$$\frac{t}{qt} = \frac{1}{K2qe2} + \frac{t}{qe} \quad (4)$$

at equilibrium, q_e is the adsorption of dye per unit mass (mg g^{-1}), qt is the mass of dye adsorbed at time t, and K1 and K2 are the rate constants for pseudo-first and pseudo-second orders. In the current research, the kinetic study was carried out at different time intervals (15 min) for MB dye adsorption. Slop and linear fit graph of log(qe–qt)against (t) and t/qt against(t) for the pseudo-first-order, and pseudo-second-order to explain the adsorption models. The intercept and slopes of the linear plots were used to calculate the values of K1, K2, and qe, respectively. A

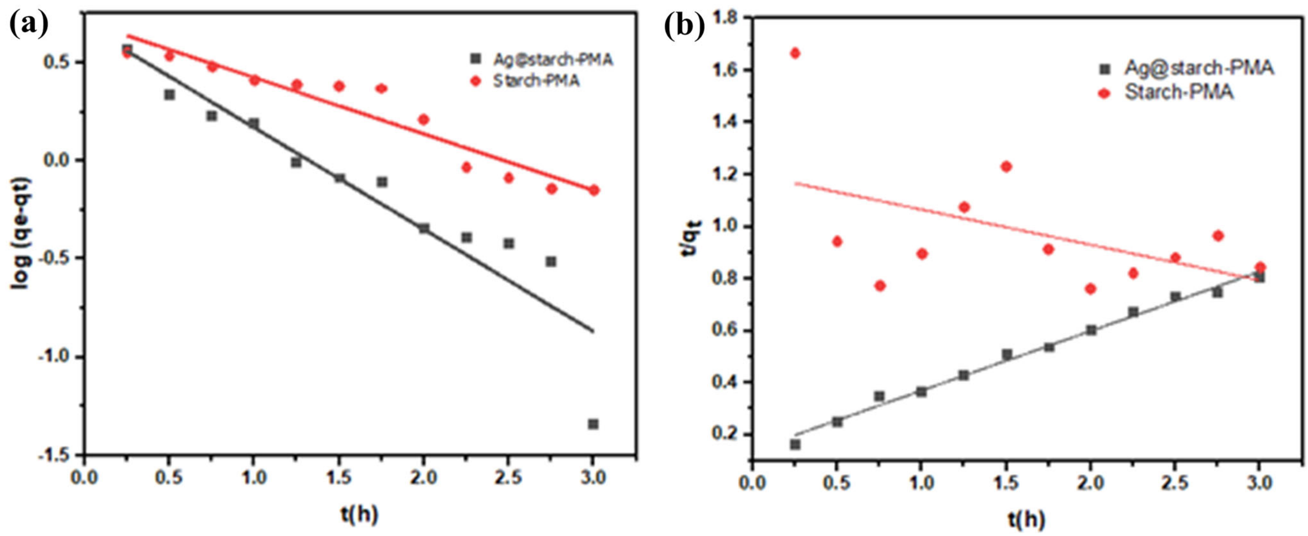

Fig. 9 Pseudo-first order and pseudo-second order plots of **a** Starch-PMA and **b** Ag@starch-PMA polymer composites

high degree of linearity in the adsorption process points to a pseudo-second-order kinetic. Pseudo-second-order kinetics had a lower correlation coefficient factor (R^2) value than pseudo-first-order kinetics. The pseudo-second-order mechanism may be used to deduce the best description of the adsorption of starch-PMA and Ag@starch-PMA for the MB aqueous solution. The correlation coefficient (R^2) and theoretical adsorption capacity values, qe, were more in accord with the actual values, qe Table 1. Therefore, the adsorption process in Fig. 9a (Starch-PMA), R^2 value 0.8619 follows the pseudo-first-order and in Fig. 9b (Ag@starch-PMA), R^2 value 0.9898 pseudo-second order kinetics for 10 ppm concentration of MB dye solution. In general, electrostatic contacts, chemical bonds, hydrogen bonds, ion exchange, van der Waal forces, and a physical adsorption process were all present in the adsorption association between adsorbents and dye. But in my current work, hydrogen bonding and electrostatic interactions between MB dye and starch-PMA, and Ag@starch-PMA polymer composites were the main factors for the adsorption process. In Table 2, the starch-PMA and Ag@starch-PMA polymer composites' ability to adsorb MB was contrasted with that of other known adsorbent materials.

3.6.3 *Adsorption isotherm study*

The relationship between adsorbent and adsorbate is extensively explained by the examination of adsorption isotherms. It is typical to use the Langmuir and Freundlich adsorption isotherms:

$$\frac{Ce}{qe} = \frac{Ce}{qm} + \frac{1}{RLqm} \tag{5}$$

$$\ln \mathrm{qe} = \ln Kf + \frac{1}{n} \ln Ce \tag{6}$$

where Ce (mg/L), qe (mg/g), and qm (mg/g) are the concentrations of MB solution, adsorption capacity, and maximum adsorption capacity at equilibrium, respectively; RL and Kf (L/mg) are the Langmuir and Freundlich constants; and n is the heterogeneity factor and quantifies the intensity of adsorption. Both models may be used to investigate the MB dye adsorption behavior of manufactured starch-PMA

Table 1 Adsorption kinetic factors for the adsorption of Methylene blue onto Starch-PMA and Ag@Starch-PMA

Concentration of dye (ppm)	Pseudo-first order			Pseudo-second order		
	K_1	Q_e	R^2	K_2	Q_e	R^2
Starch-PMA						
10	0.0104	4.29	0.8619	0.000004403	434.783	0.2356
Ag@Starch-PMA						
	0.014	2.438	0.5303	0.000102	263.16	0.9898

Table 2 Comparison of the maximal dye-removal adsorption capabilities of starch-PMA, Ag@starch-PMA, and other adsorbents

Sr No	Adsorbent	Dye	Adsorption capacity (mg/g)	References
1	BPCMC-g-poly(NaAc-co-AM)	MB	333	[51]
2	Poly(AA-co-AMPS)/montmorillonite	MB	192	[52]
3	β-CD/PAA/GO nanocomposite	MB	247	[53]
4	Cellulose nanocrystal-Alginate	MB	256	[54]
5	Polymer-modified eggshell composite	MB	345 ± 4	[55]
6	P*p*AP/Starch/GO ternary nanocomposites	MB	250.2	[56]
7	AG-CMC-AgNPnanocomposite	MB	66.68	[57]
8	Hyd and Hyd/CB	MB	26.247 and 27.32	[58]
9	Silver nanoparticles/porphyrin/reduced graphene oxide hydrogel	MB	130.37	[59]
10	starch-PMA	MB	434.783	Current study
	Ag@starch-PMA		263.16	

Table 3 Langmuir adsorption isotherms parameters

Model	Parameters	Starch-PMA	Ag@Starch-PMA
Langmuir isotherm	R^2	0.994	0.994
	q_{max} (mg/g)	522.7834	541.2563

and Ag@starch-PMA. The isotherm factors are listed in Table 3 and Fig. 10 displays the linear expression of Ce/qe against Ce for the Langmuir isotherm and lnqe against lnCe for the Freundlich isotherm, which are used to evaluate and corresponding parameters for both adsorbents, slop and intercepts ($1/q_{max}$ (slop) and $1/q_{max}$ b). It was observed that the values of the Q_{max} (mg/g) for Starch-PMA (522.7834) and Ag@Starch-PMA (541.2563) and b, respectively, were calculated using the slope and intercept of the plot. With a linear correlation value of R^2 = 0.994, the data for the MB dye adsorption onto Starch-PMA and Ag@starch-PMA polymer composites were fed into the Langmuir equation. According to the findings, the maximum adsorption (q_{max}) of MB values for Starch-PMA and Ag@Starch-PMA were 522.7834 and 541.2563, respectively.

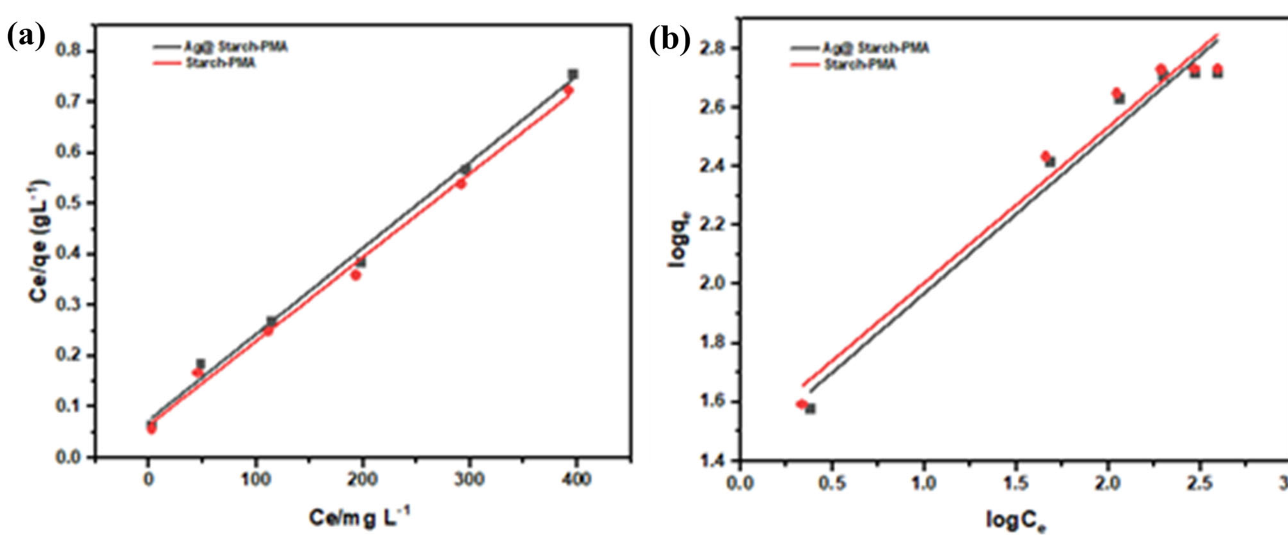

Fig. 10 Fitting curves of Langmuir isotherm model **a** Langmuir isotherm model. **b** Freundlich isotherm model

4 Conclusion

Novel starch-grafted polymer composites as adsorbents were successfully prepared via free radical polymerization. Spectroscopic techniques reveal the existence of hydroxyl and carboxylic groups on the surface of the adsorbents, and these groups are essential to the adsorptive removal of MB in the pH range of 7.4–9.4. The experimental results of MB adsorption on starch-PMA and Ag@starch-PMA support pseudo-first order and pseudo-second order, respectively, with correlation values (R^2) of 0.8619 and 0.9898. The isotherm experimental data, which depicts a homogenous monolayer on the surface of adsorbents, is the best match for the Langmuir isotherm. Moreover, the biodegradation of the polymer composites with the biodegradability value of starch-PMA 37.79% and Ag@satrch-PMA 36.92% were also confirmed using the soil burial method.

Acknowledgements

The authors are thankful to the Deanship of Scientific Research at University of Bisha for supporting this work through the Fast-Track Research Support Program. This research was funded by Princess Nourah bint Abdulrahman University Researchers Supporting Project number (PNURSP2023R7), Princess Nourah bint Abdulrahman University, Riyadh, Saudi Arabia.

Author contribution

MA: Conception, performed adsorption experiments, visualization of data, writing reviewing, and editing. AM: Material synthesis, visualization of data, writing reviewing, and editing. MJ: Analysis and/or interpretation of data, performed SEM analysis. SI: Design of study, performed major experimental works, writing-original draft preparation. RL: Methodology, reviewed original manuscript, and critical revision. MTA: Conducted XRD experiments, acquisition of data, and writing-original draft preparation. WU: Drafting the revised manuscript, performed Cu removal analysis and critical revision. RAA: Conception, FTIR analysis, acquisition of data, interpret the data. EA: Visualization of data, BET analysis, reviewed the original manuscript and critical revision. AEAF: Drafting the revised manuscript, acquisition of data, and critical revision. MMAA: Acquisition of data, reviewed original manuscript, and critical revision. EBE: Analysis and/or interpretation of data, reviewed the original manuscript and critical revision.

Funding

The authors are thankful to the Deanship of Scientific Research at University of Bisha for supporting this work through the Fast-Track Research Support Program. This research was funded by Princess Nourah bint Abdulrahman University Researchers Supporting Project number (PNURSP2023R7), Princess Nourah bint Abdulrahman University, Riyadh, Saudi Arabia.

Data availability

The datasets generated during and/or analyzed during the current study are available from the corresponding author upon reasonable request.

Declarations

Competing interest The authors declare no conflict of interest.

References

1. A.A. Elzain, M.R. El-Aassar, F.S. Hashem, F.M. Mohamed, A.S.M. Ali, Removal of methylene dye using composites of poly (styrene-co-acrylonitrile) nanofibers impregnated with adsorbent materials. J. Mol. Liq. **291**, 111335 (2019)
2. A.E. Alprol, M.S. Gaballah, M.A. Hassaan, Micro and nanoplastics analysis: focus on their classification, sources and impacts in marine environment. Reg. Stud. Mar. Sci. **42**, 101625 (2021)
3. M.R. El-Aassar, H.S. Hassan, M.F. Elkady, M.S. Masoud, A.A. Elzain, Isothermal, kinetic, and thermodynamic studies on copper adsorption on modified styrene acrylonitrile copolymer. Int. J. Environ. Sci. Technol. **16**, 7037–7048 (2019)
4. C.B. Godiya, Y. Xiao, X. Lu, Amine functionalized sodium alginate hydrogel for efficient and rapid removal of methyl blue in water. Inter. J. Bio. Macromol. **144**, 671–681 (2020)

5. S.M. Wabaidur, M.A. Khan, M.R. Siddiqui, M. Otero, B.-H. Jeon, Z.A. Alothman, A.A.H. Hakami, Oxygenated functionalities enriched MWCNTs decorated with silica coated spinel ferrite—a nanocomposite for potentially rapid and efficient decolorization of aquatic environment. J. Mol. Liq. **317**, 113916 (2020)
6. S.Z. Abbas, Y.-C. Yong, M.A. Khan, M.R. Siddiqui, A.A.H. Hakami, S.A. Alshareef, M. Otero, M. Rafatullah, Bioflocculants produced by bacterial strains isolated from palm oil mill effluent for application in the removal of Eriochrome Black T dye from water. Polymers **12**, 1545 (2020)
7. I. Hasan, I.I. BinSharfan, R.A. Khan, A. Alsalme, L-ascorbic acid-g-polyaniline mesoporous silica nanocomposite for efficient removal of crystal violet: a batch and fixed bed breakthrough studies. Nanomaterials **10**, 2402 (2020)
8. M.X. Zhu, L. Lee, H.H. Wang, Z. Wang, Removal of an anionic dye by adsorption/precipitation processes using alkaline white mud. J. Hazard Mater. **149**, 735–741 (2007)
9. A. Akbari, J.C. Remigy, P. Aptel, Treatment of textile dye effluent using a polyamide-based nanofiltration membrane. Chem. Eng. Process **41**, 601–609 (2002)
10. M. Rastgar, A.R. Zolfaghari, H.R. Mortaheb et al., Photocatalytic/adsorptive removal of methylene blue dye by electrophoretic nanostructured TiO2/montmorillonite composite flms. J. Adv. Oxid. Technol. **16**, 292–297 (2013)
11. D.Y. Zhou, G.Z. Wang, W.S. Li, G.L. Li, C.L. Tan, M.M. Rao, Y.H. Liao, Preparation and performances of porous polyacrylonitrile-methyl methacrylate membrane for lithium-ion batteries. J. Power Sources **184**, 477–480 (2008)
12. A.E. Al Prol, Study of environmental concerns of dyes and recent textile effluents treatment technology: a review. Asian J. Fish. Aquat. Res. **3**, 1–18 (2019)
13. M.S. MohyEldin, M.A. Abu-Saied, T.M. Tamer, M.E. Youssef, A.I. Hashem, M.M. Sabet, Development of polystyrene based nanoparticles ions exchange resin for water purification applications. Desalin. Water Treat. **57**, 14810–14823 (2016)
14. C. Pelekani, V.L. Snoeyink, Kinetic and equilibrium study of competitive adsorption between atrazine and Congo red dye on activated carbon: the importance of pore size distribution. Carbon N Y **39**, 25–37 (2001)
15. P. Pendleton, S.H. Wu, Kinetics of dodecanoic acid adsorption from caustic solution by activated carbon. J. Colloid Interface Sci **266**, 245–250 (2003)
16. P.C.C. Faria, J.J.M. Orfao, M.F.R. Pereira, Adsorption of anionic and cationic dyes on activated carbons with diferent surface chemistries. Water Res **38**, 2043–2052 (2004)
17. L. Ai, M. Li, L. Li, Adsorption of methylene blue from aqueous solution with activated carbon/cobalt ferrite/alginate composite beads: kinetics, isotherms, and thermodynamics. J Chem Eng Data **56**, 3475–3483 (2011)
18. M.A. Khan, M.R. Siddiqui, M. Otero, S.A. Alshareef, M. Rafatullah, Removal of rhodamine b from water using a solvent impregnated polymeric dowex 5wx8 resin: statistical optimization and batch adsorption studies. Polymers **12**, 500 (2020)
19. E.I. Unuabonah, A. Taubert, Clay–polymer nanocomposites (CPNs): adsorbents of the future for water treatment. Appl. Clay Sci. **99**, 83–92 (2014)
20. C.B. Godiya, L.A.M. Ruotolo, W. Cai, Funtional biobased hydrogels for the removal of aqueous hazardous pollutants: current status, challenges and future perspectives. J. Mater. Chem. A **8**, 21585–21612 (2020)
21. M. Yusuf, M. Kumar, M.A. Khan, M. Sillanpää, H. Arafat, A review on exfoliation, characterization, environmental and energy applications of graphene and graphene-based composites. Adv. Colloid Inter. Sci. **273**, 102036 (2019)
22. K. Rahimi, R. Mirzaei, A. Akbari, N. Mirghaffari, Preparation of nanoparticle-modified polymeric adsorbent using wastage fuzzes of mechanized carpet and its application in dye removal from aqueous solution. J. Cleaner Prod. **178**, 373–383 (2018)
23. M.H. Baek, C.O. Ijagbemi, O. Se-Jin, D.S. Kim, Removal of malachite green from aqueous solution using degreased cofee bean. J Hazard Mater **176**, 820–828 (2010)
24. M. Zhao, Z. Tang, P. Liu, Removal of methylene blue from aqueous solution with silica nano-sheets derived from vermiculite. J Hazard Mater **158**, 43–51 (2008)
25. A.A. Attia, B.S. Girgis, N.A. Fathy, Removal of methylene blue by carbons derived from peach stones by H3PO4 activation: batch and column studies. Dye Pigment **76**, 282–289 (2008)
26. S. Hajati, M. Ghaedi, H. Mazaheri, Removal of methylene blue from aqueous solution by walnut carbon: optimization using response surface methodology. Desalin. Water Treat **57**, 3179–3193 (2016)
27. S. Ahmad, M. Ahmad, K. Manzoor et al., A review on latest innovations in natural gums based hydrogels: preparations and applications. Int J Biol Macromol **136**, 870–890 (2019)
28. S. Iqbal, S. Nadeem, R. Bano, A. Bahadur, Z. Ahmad, M. Javed, M.A. Qayyum, Green synthesis of biodegradable terpolymer modified starch nanocomposite with carbon nanoparticles for food packaging application. J. Appl. Polym. Sci. **138**(25), 50604 (2021)
29. H. Mittal, R. Jindal, B.S. Kaith et al., Synthesis and foccu-lation properties of gum ghatti and poly(acrylamide-co-acrylonitrile) based biodegradable hydrogels. CarbohydrPolym **114**, 321–329 (2014)

30. J. Singh, A.S. Dhaliwal, Novel green synthesis and characterization of the antioxidant activity of silver nanoparticles prepared from Nepeta leucophylla root extract. Anal. Lett. **52**, 213–230 (2019)
31. S. Ghorai, A. Sarkar, M. Raouf et al., Enhanced removal of methylene blue and methyl violet dyes from aqueous solution using a nanocomposite of hydrolyzed polyacrylamide grafted xanthan gum and incorporated nanosilica. ACS Appl. Mater. Interfaces **6**, 4766–4777 (2014)
32. H. Mittal, A. Maity, S.S. Ray, Gum karaya based hydrogel nanocomposites for the efective removal of cationic dyes from aqueous solutions. Appl. Surf. Sci. **364**, 917–930 (2016)
33. D.C. Manatunga, R.M. De Silva, K.M.N. De Silva, R. Ratnaweera, Natural polysaccharides leading to super adsorbent hydroxyapatite nanoparticles for the removal of heavy metals and dyes from aqueous solutions. RSC Adv. **6**, 105618–105630 (2016)
34. E.F. Lessa, A.L. Medina, A.S. Ribeiro, A.R. Fajardo, Removal of multi-metals from water using reusable pectin/cellulose microfibers composite beads. Arab. J. Chem. **13**, 709–720 (2020)
35. R. Sharma, S. Kalia, B.S. Kaith, M.K. Srivastava, Synthesis of guar gum-acrylic acid graft copolymers based biodegradable adsorbents for cationic dye removal. Int. J. Plast. Technol. **20**, 294–314 (2016)
36. N. Amirmahani, H. Mahdizadeh, N. Seyedi, A. Nasiri, G. Yazdanpanah, Synthesis and performance evaluation of chitosan/zinc oxide nanocomposite as a highly efficient adsorbent in the removal of reactive red 198 from water. J. Chin. Chem. Soc. (2021). https://doi.org/10.1002/jccs.202200514
37. M. Malakootian, J. Smith, M. Gharaghani, H. Mahdizadeh, A. Nasiri, G. Yazdanpanah, Decoloration of textile acid red 18 dye by hybrid UV/COP advanced oxidation process using ZnO as a catalyst immobilized on a stone surface. Desalin. Water Treat. **182**, 385–394 (2020)
38. A.A. Menazea, N.S. Awwad, Pulsed Nd: YAG laser deposition-assisted synthesis of silver/copper oxide nanocomposite thin film for 4-nitrophenol reduction. Radiat. Phys. Chem. **177**, 109112 (2020)
39. F.J. Warren, M.J. Gidley, B.M. Flanagan, Infrared spectroscopy as a tool to characterise starch ordered structure—a joint FTIR-ATR, NMR, XRD and DSC study. Carbohydr. Polym. **139**, 35 (2016)
40. S. Iqbal, S. Nadeem, A. Bahadur, M. Javed, Z. Ahmad, M.N. Ahmad, M. Shoaib, G. Liu, A. Mohyuddin, M. Raheel, JOM **73**, 380 (2021)
41. S. Iqbal, A. Bahadur, S. Ali, Z. Ahmad, M. Javed, R.M. Irfan, N. Ahmad, M.A. Qamar, G. Liu, M.B. Akbar, M. Nawaz, J. Alloys Compd. **858**, 158338 (2021)
42. S. Iqbal, M. Javed, A. Bahadur, M.A. Qamar, M. Ahmad, M. Shoaib, M. Raheel, N. Ahmad, M.B. Akbar, H. Li, J. Mater. Sci. Mater. Electron. **31**, 842 (2020)
43. S. Iqbal, N. Ahmad, M. Javed, M.A. Qamar, A. Bahadur, S. Ali, Z. Ahmad, R.M. Irfan, G. Liu, M.B. Akbar, M.A. Qayyum, J. Environ. Chem. Eng. **9**, 104919 (2021)
44. M.N. Siddiqui, H.H. Redhwi, L. IoannisTsagkalias, C. Softas, M. Ioannidou, D. Achilias, Synthesis and characterization of poly (2-hydroxyethyl methacrylate)/silver hydrogel nanocomposites prepared via in situ radical polymerization. Thermochim Acta **643**, 53–64 (2016)
45. R. Xu, J. Mao, N. Peng, X. Luo, C. Chang, Chitin/clay microspheres with hierarchical architecture for highly efficient removal of organic dyes. Carbohydr. Polym. **188**, 143–150 (2018)
46. G. Zhou, J. Luo, C. Liu, L. Chu, J. Crittenden, Efficient heavy metal removal from industrial melting effluent using fixed-bed process based on porous hydrogel adsorbents. Water Res. **131**, 246–254 (2018)
47. G. Zhou, J. Luo, C. Liu, L. Chu, J. Ma, Y. Tang, S. Luo, A highly efficient polyampholyte hydrogel sorbent based fixed-bed process for heavy metal removal in actual industrial effluent. Water Res. **89**, 151–160 (2016)
48. K. Sharma, B.S. Kaith, V. Kumar, S. Kalia, V. Kumar, H.C. Swart, Water retention and dye adsorption behavior of Gg-cl-poly (acrylic acid-aniline) based conductive hydrogels. Geoderma **232**, 45–55 (2014)
49. S. Chen, J. Wang, Z. Wu, Q. Deng, W. Tu, G. Dai, S. Deng, Enhanced Cr (VI) removal by polyethylenimine-and phosphorus-codoped hierarchical porous carbons. J. Colloid Interface Sci **523**, 110–120 (2018)
50. W. Zhang, S. Zhang, J. Wang, M. Wang, Q. He, J. Song, J. Zhou, Hybrid functionalized chitosan-Al2O3@ SiO2 composite for enhanced Cr (VI) adsorption. Chemosphere **203**, 188–198 (2018)
51. K. Bello, B.K. Sarojini, B. Narayana, A. Rao, K. Byrappa, A study on adsorption behavior of newly synthesized banana pseudo-stem derived superabsorbent hydrogels for cationic and anionic dye removal from effluents. Carbohyd. Polym. **181**, 605–615 (2018)
52. H. Hosseinzadeh, N. Khoshnood, Removal of cationic dyes by poly (AA-co-AMPS)/montmorillonite nanocomposite hydrogel. Desalin. Water Treat. **57**(14), 6372–6383 (2016)
53. J. Liu, G. Liu, W. Liu, Preparation of water-soluble β-cyclodextrin/poly (acrylic acid)/graphene oxide nanocomposites as new adsorbents to remove cationic dyes from aqueous solutions. Chem. Eng. J. **257**, 299–308 (2014)
54. N. Mohammed, N. Grishkewich, R.M. Berry, K.C. Tam, Cellulose nanocrystal–alginate hydrogel beads as novel

adsorbents for organic dyes in aqueous solutions. Cellulose **22**(6), 3725–3738 (2015)

55. O.A. Bin-Dahman, T.A. Saleh, Synthesis of polyamide grafted on biosupport as polymeric adsorbents for the removal of dye and metal ions. Biomass Conv. Bioref. (2022). https://doi.org/10.1007/s13399-022-02382-8
56. H.K. Ismail, L.I.A. Ali, H.F. Alesary, B.K. Nile, S. Barton, Synthesis of a poly (p-aminophenol)/starch/graphene oxide ternary nanocomposite for removal of methylene blue dye from aqueous solution. J. Polym. Res. **29**(5), 159 (2022)
57. S.I. Mostafa, M.A. Ali, N.A. El-Wassefy, E.M. Saad, M.H. Hussein, Adsorption and interaction studies of methylene blue dye onto agar-carboxymethylcellulose-silver nanocomposite in aqueous media. Biomass Conv. Bioref. (2022). https://doi.org/10.1007/s13399-022-02505-1
58. S.J. Peighambardoust, E. Ghergherehchi, P. Mohammadzadeh Pakdel, H. Aghdasinia, Facile removal of methylene blue using carboxymethyl cellulose grafted polyacrylamide/carbon black nanocomposite hydrogel. J. Polym. Environ. **31**(3), 939–953 (2023)
59. A.L.T. Zheng, T. Phromsatit, S. Boonyuen, Y. Andou, Synthesis of silver nanoparticles/porphyrin/reduced graphene oxide hydrogel as dye adsorbent for wastewater treatment. FlatChem **23**, 100174 (2020)

Publisher's Note Springer Nature remains neutral with regard to jurisdictional claims in published maps and institutional affiliations.